

CCN Spectral Shape Effects on Cloud Microphysics and Drizzle

Hudson and Noble, DRI

Three cloud processes cause bimodal particle size and CCN distributions by increasing the mass of dissolved material within cloud droplets, which upon evaporation are larger and thus size and S_c -separated from particles that did not produce cloud droplets.

- 1) Coalescence among droplets;
- 2) Gas-to-particle chemical reactions, e.g., sulfate and nitrate;
- 3) Brownian capture of interstitial material.

Since these cloud processes do not affect unactivated particles a gap in the dry particle size distribution or CCN spectra occurs when droplets evaporate, as they usually do. The larger size mode (> 100 nm, lower S_c) that has usually been cloud processed is the accumulation mode while the cloud unprocessed smaller mode (< 100 nm, higher S_c) is the Aitken mode.

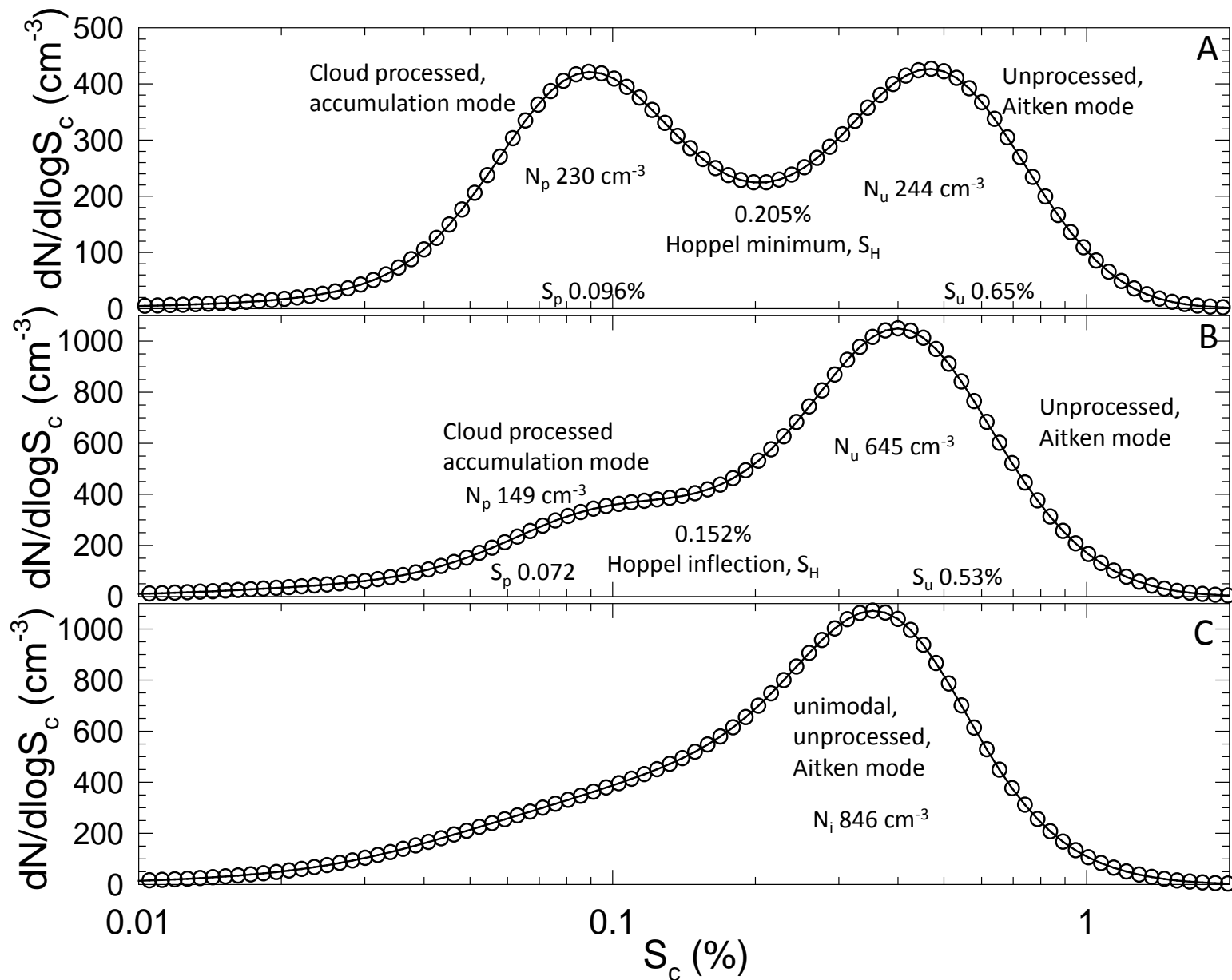


Figure 1. Examples of bimodal and unimodal CCN spectra observed during MASE off the central California coast, polluted summertime stratus.

One way to characterize CCN modality, i.e., shape of the spectra, is according to the slope of traditional cumulative spectra plotted log-log, k .

For the low cloud supersaturations, S , observed during MASE the relevant critical S , S_c , range was 0.5-0.1%.

Unimodal spectra, smaller Aitken particles with high S_c that are not cloud processed exhibit high k .

Bimodal spectra, Aitken and accumulation particles, unprocessed and processed, exhibit lower k .

During MASE we examined 130 sets of CCN spectra and associated cloud parcel microphysics during horizontal passes above the CCN during eight research flights over a nine-day period of July, 15-23.

All data were put into order according to $k(0.5-0.1\% S_c)$. Data were then divided into equal, halves, quartiles, and octiles. Halves and extreme quartiles and octiles were examined.

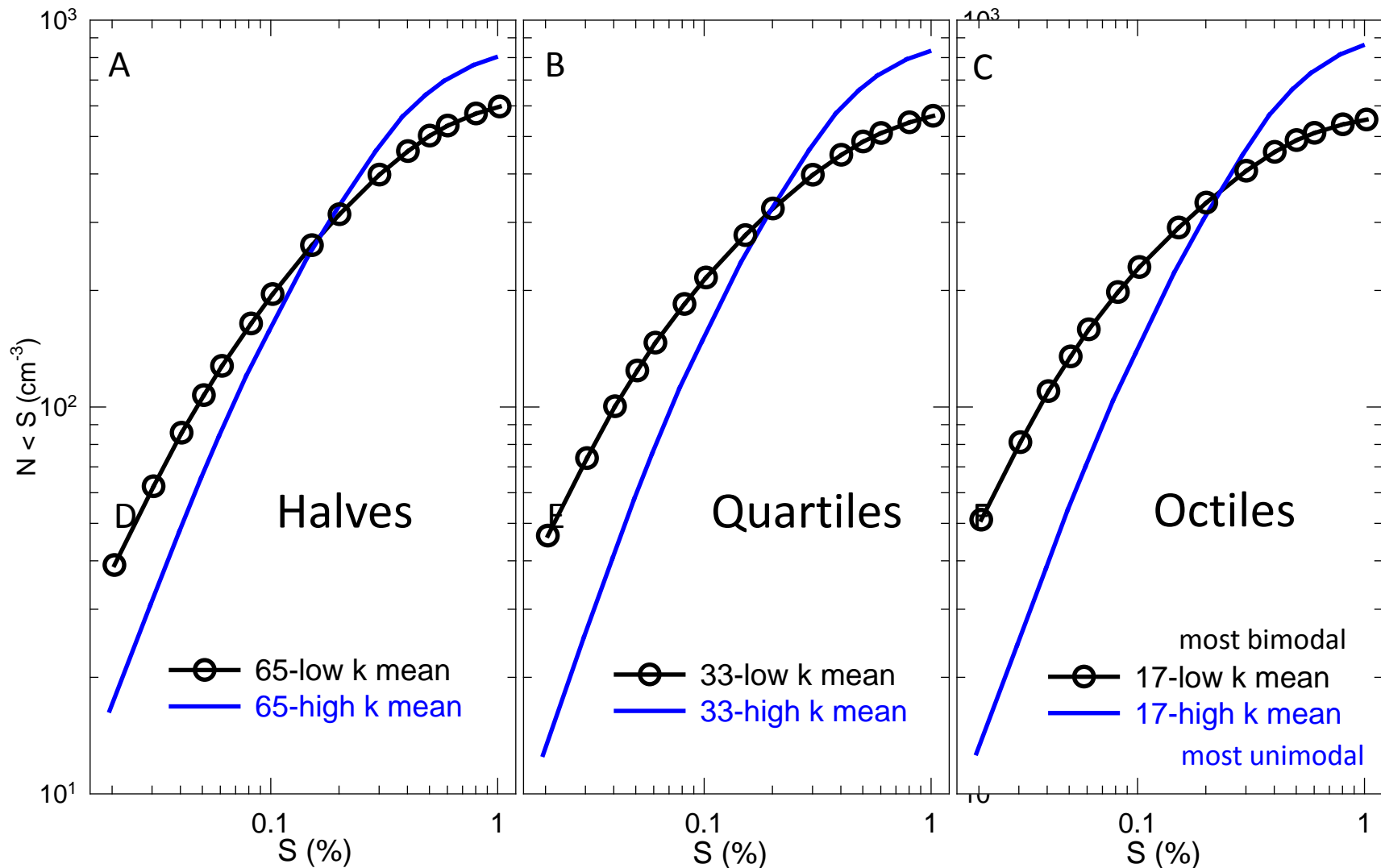


Figure 2. Means of cumulative CCN spectra plotted log-log for the six divisions noted in the legends.

Greater concentration differences with S for higher k unimodal spectra.

	A 65 lowest	B 65 highest	C 33 lowest	D 33 highest	E 17 lowest	F 17 highest
k(0.5-0.1%)	0.62	0.98	0.52	1.04	0.48	1.09
N_c (cm ⁻³)	274	214	309	195	340	193
MD (μm)	8.71	9.87	8.06	10.31	7.26	10.39
σ (μm)	3.84	4.73	3.58	5.24	3.60	5.30
N_d (liter ⁻¹)	2.60	5.89	1.23	7.01	0.70	7.44

Table 1. Means of 130 CCN and associated cloud data divided into halves (A and B), quartiles (C and D), and octiles (E and F) according to CCN k(0.5-0.1%), the log-log slope of the cumulative CCN spectra between 0.5 and 0.1% S; only the two extreme quartiles and octiles are shown. N_c -cloud droplet concentration, MD-mean diameter of cloud droplet spectra, σ -standard deviation of cloud droplet spectra, N_d -drizzle drop concentration. Higher values in the two adjacent columns are bold.

Cloud processing reduces k, increases droplet concentration, decreases droplet sizes, narrows droplet spectra, and reduces drizzle. Similar results for various cloud thresholds.

	thhold	R	P2	thhold	R	P2	thhold	R	P2
N_c	0.10	-0.42	0.077	0.05	-0.44	0.057	no	-0.40	0.088
MD	0.10	+0.36	0.131	0.05	+0.44	0.059	no	+0.41	0.084
σ	0.10	+0.57	0.012	0.05	+0.60	0.006	no	+0.61	0.006
N_d	0.10	+0.61	0.006	0.05	+0.53	0.020	no	+0.52	0.023

Table 2. Correlation coefficients (R) and two-tailed probabilities (P2) for slope of cumulative spectra (k) between 0.5 and 0.1% S, with four cloud and drizzle characteristics for 19 clouds using 0.10 and 0.05 g/cm³ LWC_c threshold and no cloud threshold.

Entrainment or non-adiabaticity does not perturb these relationships.

More diverse CCN spectra of unimodal unprocessed CCN with higher k yields more diverse droplet spectra, higher σ .

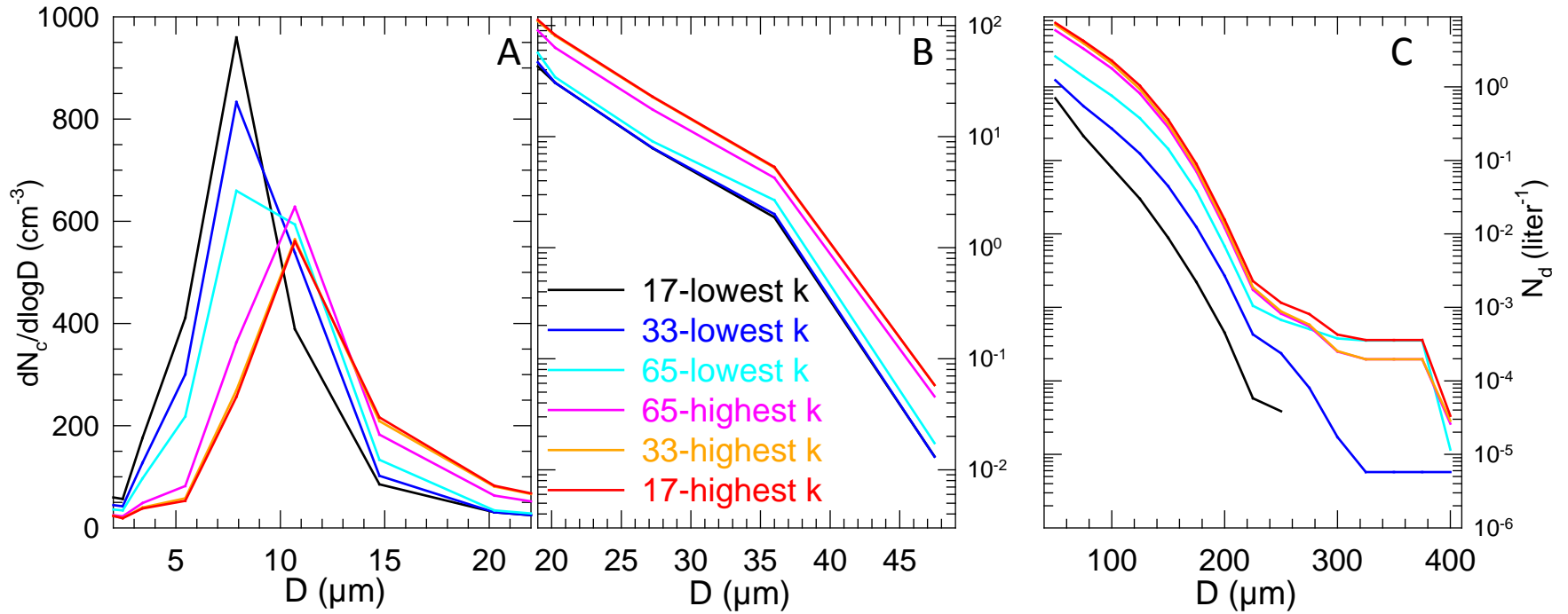


Figure 3. (A and B). Mean differential droplet concentrations against diameter for clouds associated with six divisions of data according to the slopes of log-log cumulative CCN spectra, k . **(C)** As A and B, but considering cumulative drizzle drop concentrations, N_d .

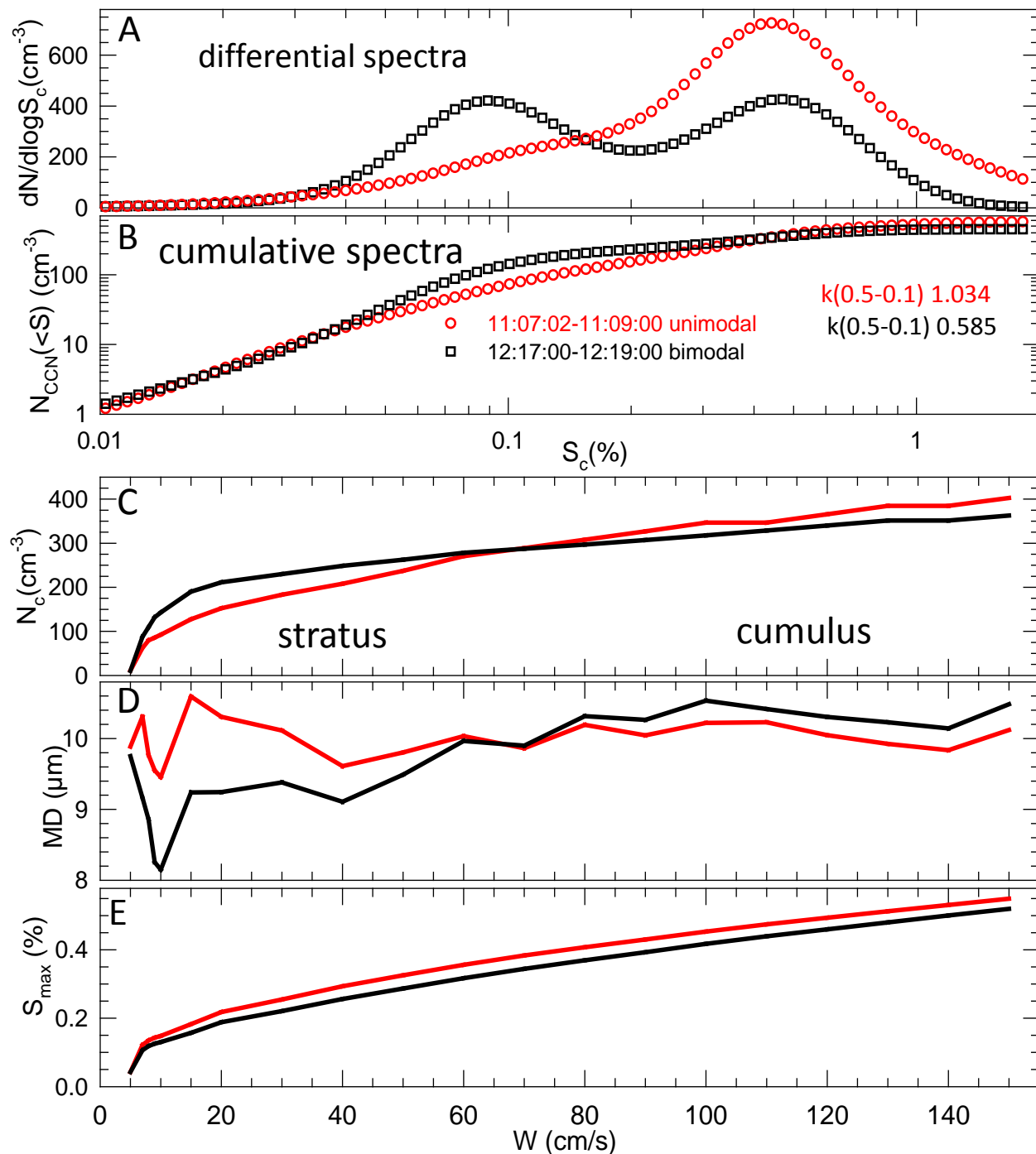


Figure 4. (A) and (B) are measured CCN spectra of 15 July, 2005. (A) is differential and (B) is cumulative presentation with slopes, k . C-E are cloud microphysics predictions by an adiabatic model at the same distances above cloud base for clouds grown on each CCN spectrum with various vertical winds (W) applied to these two CCN spectra. (C) Shows cloud droplet concentrations. (D) is the mean diameter of the cloud droplet spectra. (E) is the resulting supersaturation.

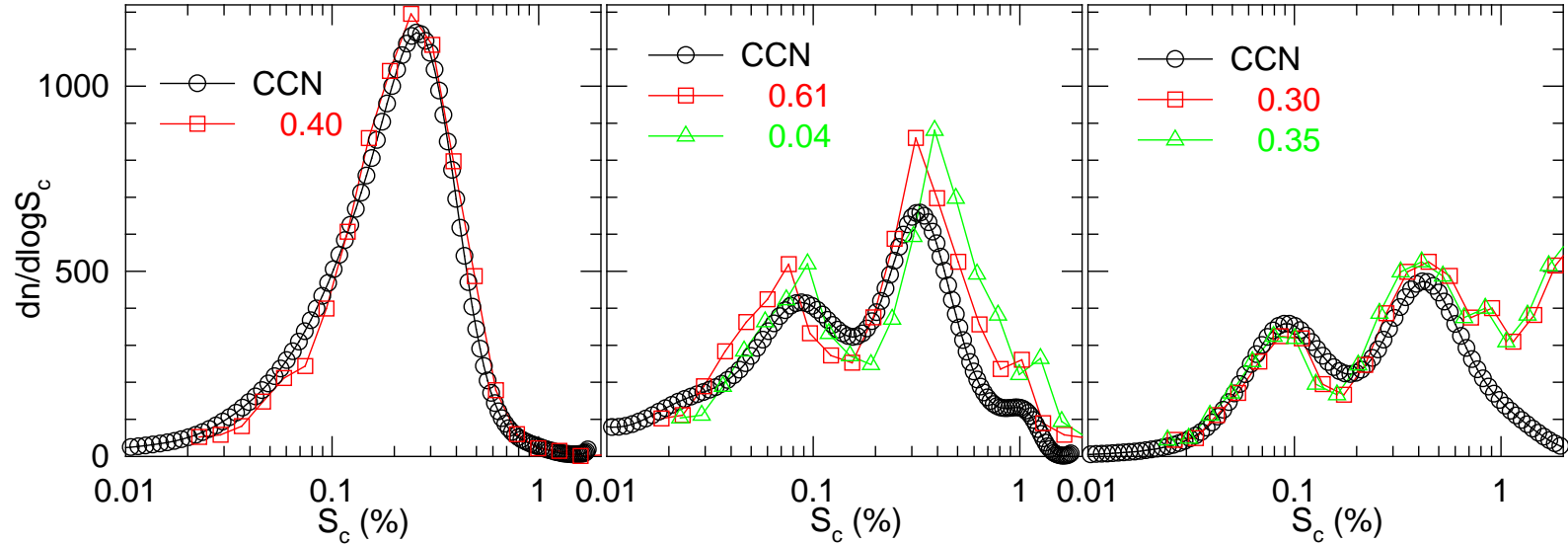


Figure 5. MASE below cloud examples of simultaneous CCN (black) and DMA (red and green) distributions. Hygroscopicity, κ , in legend converts DMA size to critical supersaturation, S_c . Higher S_c are smaller particles. Lower S_c are larger particles.

Can obtain κ continuously without interrupting continuous ambient CCN and dry particle spectra.

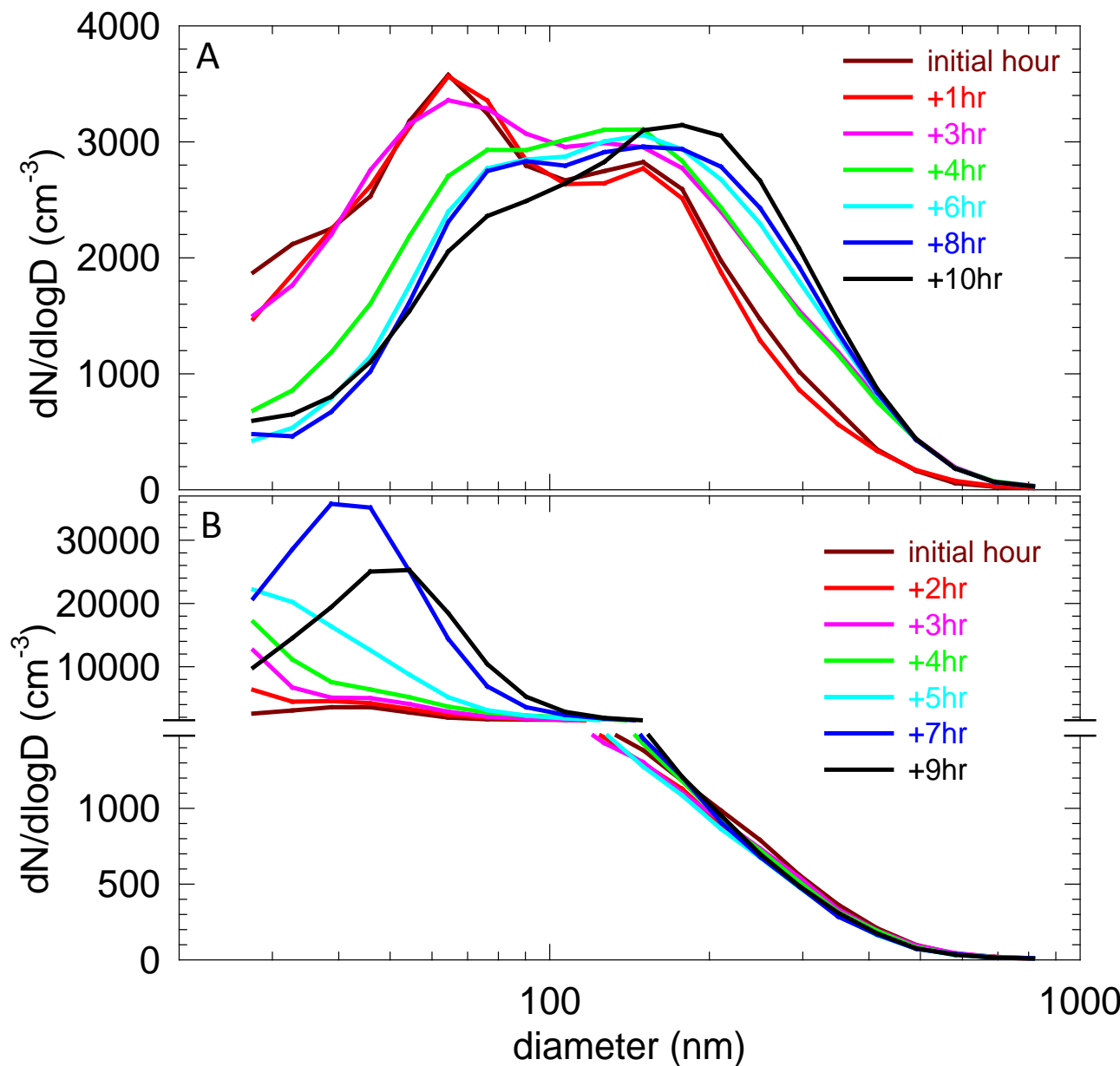


Figure 6. At SGP surface. Mean particle size distributions at the initial onset of 7+ consecutive hours of **A**) ceilometer cloud fraction > 0.75 when mixing height > cloud base altitude and the majority of hours are daytime; and **B**) daytime ceilometer cloud fraction = 0.. Hours following onset are denoted in legend.

Cloud processing happens over continents. Also observe photochemical particle production in clear skies.

Poster 88 and presentation tomorrow afternoon.

Conclusions for MASE stratus:

1. Cloud processing reduces k , the slope of CCN spectra.
2. Cloud processing makes more cloud droplets.
3. With smaller mean sizes.
4. And narrower spectra.
5. And less drizzle.
6. These enhancements of 1st and 2nd IAE are above and beyond original IAE due to higher CCN concentrations of air pollution.
7. These effects seem similar to that of higher CCN concentrations but they are a result of differences in CCN spectral shape.